

# Index

Page numbers in *italic* denote figures. Page numbers in **bold** denote tables.

- abiotic method 377
- aborted reversals 4, 5, 6
  - outer Great Barrier Reef 279
- Pringle Falls 261, 262, 270–271, 273–275
- accretion 193
- acquisition behaviour 16
- Adriatic Promontory 112
- aeolian component 378, 379, 387, 389
  - dust proxy 326, 333–335, 336, 338
- AF *see* alternating-field demagnetisation
- age control, magnetostratigraphy 138, **139**, 141, 142, 144, 145
- age-depth model 247
  - Lake Kalimpaa 250, 254–257
  - Nankai Trough 229–230, 232–240
  - ODP Hole 711A 105, 107
  - Stirone section 317–320
- air-fall volcanic ash 112, 123, 193, 194–195
- Alashan Block 150, 152, 186
- alloycyclic forcing mechanism 325
- alternating-field demagnetisation
  - Cupido Formation, Mexico 330, 331
  - IODP Site U1333 17, 18
  - Lake Kalimpaa 251, 253
  - Monte Cagnero 83, 84
  - Nankai Trough 192–193, 195, 197, 198, 199, 223
  - ODP Hole 647A 32, 33, 34
  - ODP Hole 711A 100, 101, 103
  - outer Great Barrier Reef 287, 288
  - Pringle Falls 266, 268
  - Stirone section 312, 313, 314, 315
  - Tibetan Plateau 156
- AMS *see* anisotropy of magnetic susceptibility
- analysis methods, magnetic cyclostratigraphy 329–330
- anhysteretic remanent magnetization 6–7, 15, 16, 18
  - as palaeoclimate proxy 326
  - Cretaceous 330, 331–337
  - Holocene 248, 252, 254
  - Permian 378
  - Pliocene–Pleistocene 309, 316
- anisotropic behaviour 294, 346
- anisotropy in geomagnetic trajectories 303, 306
- anisotropy of magnetic susceptibility 6, 262
- anisotropy of magnetic susceptibility in rhythmites 355–370
  - data and methods 358, 360
  - sediment transport 357
  - tensor axes 360, 364
- anoxic conditions 321
- Antarctic glaciation 98–99
- Apache Mountains sections 377, 379, 384, 385, 387–390
- Apennines (Northern), cyclostratigraphy 309–321
- Apparent Polar Wander Path 6
- Ar/Ar date 275, 288, 294
- archives, Lake Kalimpaa 247
- ARM *see* anhysteretic remanent magnetization
- astrochronology 328
- astronomical calibration **368**, 370, 379
  - astronomical forcing cycles 7–8
  - astronomical harmonic features 355, 363–367
  - astronomical parameters 360
  - astronomical signal, Garcia Canyon 335–336, 338
  - astronomical time scale 341
  - Atlantic (NW), circulation 30
  - atmospheric circulation 334, 338
  - atmospheric CO<sub>2</sub> 377
  - Australia, dating latest Holocene 247
  - authigenic ferromagnetic minerals 344
  - auto-cyclic forcing mechanism 325
- backarc spreading 193
- bacteria 343, 344
- bar-log format 345, 346, 348, 380, 381, 382
- Bayesian inversion 295, 297
- bentonite 112
- bioevents 91–92
  - foraminifera 85, 87–89
  - nanofossils 88–89, **99**, 103, 105
- biogenic components 343
- biogenic magnetite 287–288
- biomagnetostratigraphy, integration high to low latitudes 29–74
- biosilica accumulation rate 68, 69, 71
- biostratigraphic and palaeomagnetic age datum **233–235**, **237–239**
  - Magnetic Reversal Polarity Timescale *Fig.10*
  - opposite page 56
- biostratigraphy
  - Cretaceous 327–328
  - ODP Hole 647A 34–38, 39–47, **48–49**
  - ODP Hole 711A 105–206
  - Palaeogene 113–114, 121
  - Permian, Mid 376–377, 389–390
  - Pleistocene 311, 313, 316
- biotite-rich layer 112, 123
- Blake event 262
- Blake excursion 288, 289
- block-floating model 169
- Bond cycle 367
- bootstrap method 157, 159
- Brazilian lavas, virtual geomagnetic pole paths 293–306
- Brunhes Chron correlation 273–274, 275
- Brunhes Chron excursion 288
- bulk low-field mass specific magnetic susceptibility 341, 343
- calcarenite 312, 316, 319, 320
- calcite compensation depth 97, 98, 107
- Capitanian, global stratotype 376, 384, 385, 387, 390, 392
- carbonate 107, 112, 343
- carbonate cyclostratigraphy 309
- carbonate platforms, cyclicity 325–329, 332–338
- carbonate sediments, magnetostratigraphy 280, 282
- carbonate–carbonate-free correlation 32, 68, 69, 71, 72

- carbonates, pelagic 82, 112–113, *116, 118*, 119–121  
 characteristic remanent magnetization (ChRM) 3  
   Guide Basin 137, 138, *140*  
   Jiuquan Basin 177–178, 180  
   Lake Kalimpa 248  
   Monte Cagnero 83, 87, 89, 100, *103, 105*  
   Nankai Trough 192–193, 195–199, 223, 226, 236,  
     240–241  
   ODP Hole 647A 34  
   outer Great Barrier Reef 287, 289  
   Pringle Falls 265–266  
   rhythmites 356, 360  
   Stirone section 312, 313  
   Tibetan Plateau 157–158  
 chemical remanent magnetization 3  
 chemoherm 311, 312, 318, 319  
 Chico Canyon 326–327, *331–333*  
 ChRM *see* characteristic remanent magnetization  
 chronology, magnetism and age 280  
 chronology, radiocarbon 250, 252–253  
 chrons 3–4, 273–275  
   ODP Hole 647A 50–65  
 chronstratigraphy and magnetostratigraphy  
   susceptibility 379  
 climate and geology 247–248, 326  
 climate cycles in susceptibility values 343–346,  
   348, 378  
 climate cycles, encoding 320–321  
 climate proxy 8, 309, 326–327, 341–342, 370, 379  
 climate, Cenozoic 13  
   Eocene–Oligocene 79, 81, 92, 97–99  
 climate-driven cycles 351  
 coal 152  
 coercivity 196  
   Lake Kalimpa 250, 254  
   outer Great Barrier Reef 282, 283  
   Pringle Falls 264–265  
 Colleen Canyon section 383, 385–387, 392  
 collision, India–Asia 8, 151, 152, 166, *167*, 168, 173  
 collision, Proterozoic 152  
 condensed sequence 325, 337, 348, 351  
 Contessa, pelagic succession 112–117, *119*, 121  
 cooling 81, 151  
 coral reef 280  
 coring, disturbance 196–197  
 correlation, ODP Hole 711A to GPTS 106  
 couplet thickness 358, *361*, *362*, 370  
 Cretaceous–Palaeogene boundary 117, 344  
   integrated chronostratigraphy 111  
 crust, flow 151  
 crust-floating model 167–169  
 Cupido Formation, magnetic cyclostratigraphy  
   325–338  
   analysis methods 329–330  
   anhysteretic remanent magnetization 331–337  
   magnetic mineralogy 330–331  
   sample collection 329  
   stratigraphy 326–328, *329*  
   time series methods 330  
 Curie point 280, 282, 287  
 Curie temperature 264, 265, 282, 285  
   determination 199, 223–224, 225, **227**  
 cyanobacteria 343  
 cyclostratigraphy 309–321, 325–338  
   data analysis, magnetostratigraphy 196–197  
   dating and geomagnetics 2, 3–6, 8  
     *see also* palaeomagnetic  
   Day plot 254, 265, 266  
   debris flow 163, 166, 167  
   declination 8, 21, 22–23, 24, 196  
     and age 185, 186  
     Lake Kalimpa 252, 255, 256  
     magma flows 296  
     outer Great Barrier Reef 287, 288–289  
     Pringle Falls 67–269, 270–271  
   deep-sea sediments, magnetostratigraphy 13–26  
   deformation and magnetostratigraphy 149–169  
   deformation rates, Quaternary 173  
   deformation, timing of 241  
   Delaware Mountains 377, 392  
   demagnetization 18, 20  
   demagnetization experiments 197–199, 265–268  
   denudation rate 146  
   deposition period, rhythmites **369**  
   depositional cyclicity, anhysteretic remanent  
     magnetization 336–337  
   depositional environment  
     Guide Basin 135, 145  
     Jiuquan Basin 181  
   depositional hiatus, Stirone section 321  
   depth scale 20, 22  
   detrital component 378, 379, 380, 387, 389  
   detrital remanent magnetization 3  
   diagenesis 6, 321, 381  
     and magnetic susceptibility 344  
   diamagnetism 379, 384  
   diatomaceous sediments 263, 266, 275  
   diatoms, ODP Hole 647A 34, **49**, 65  
   dinocyst marker species **43–44**, 56  
   dinoflagellate cysts  
     ODP Hole 647A 34  
     Umbria–Marche 113, *116, 118–120*, 121, 128  
   dipolar field 294, 303  
   dipole field, diminution 274–275  
   directional records, polarity excursions 262  
   drilling-induced magnetization 197, 199  
   drilling-induced remagnetization 34  
   dropstones, Permo–Carboniferous 357, 358, 359  
   dynamo model 294  
  
 earthquakes 191–192, 193  
 eccentricity 7, 326, **367**, **368**, 387, 388  
   orbital 335, 337, 338  
 eccentricity cycle 72  
   Ordovician 342, 347, 348  
     identified at outcrop 350, 351  
   Permian 360, 363, 379, 392  
   Pliocene–Pleistocene 315, 317, 320  
 El Nino Southern Oscillation 245  
 environment proxy 326, 333–335, 338, 356, 366  
   *see also* aeolian and climate  
 environmental magnetism 6–7  
 Eocene Thermal Maximum 73  
 Eocene–Oligocene boundary 81–82, 89,  
   90, 98, 107  
   North Atlantic 31, 35, 57, 71–72  
 Eocene–Oligocene Climatic Optimum *Fig. 10*  
   opposite page 56

- Eocene–Oligocene Transition 8, 30, 71, 73  
 geology 31, 35  
 eolian *see* aeolian  
 eustacy 325, 341, 344, 346, 378, 380  
 evaporite 327, 367  
 excursions 4, 5, 6  
 equatorial Pacific 24–26  
 Icelandic 302  
 outer Great Barrier Reef 279, 287–289  
 excursions, Pringle Falls 261–275  
 Brunhes Chron correlation 273–274, 275  
 demagnetization experiments 265–268  
 hysteresis experiments 264–265, 266  
 rock magnetic experiments 264–269  
 sampling procedure 263–264  
 virtual geomagnetic pole paths 269–274  
 extinction, *Hantkenina* spp 72  
 extinction, mass 344, 377
- facies analysis, magnetostratigraphy 133, 142–146  
 fence diagrams in magnetostratigraphy 133–146  
 ferromagnetic grains 329, 378  
 field sampling method, magnetostratigraphy 379  
 Fischer plot 157, 159, 329, 332  
 fission-track data 226, 232, 236, 240  
 floating-point time scale model 387–391  
 foraminifera  
 Eocene–Oligocene 83, 85, 87–88  
 Palaeogene 113–127  
 deep sea 35, 38, 48–49, 66  
 Pliocene–Pleistocene 318  
 foreland basin 150, 152, 163, 165, 166, 169  
 fossil mammals 135, 158, 160  
 Fourier phase estimator 301  
 Fourier transform results  
 Middle Permian 380–382, 387, 388–389, 390  
 Ordovician 347, 348
- GAD *see* geocentric axial dipole  
 gamma-ray attenuation density data 70, 71  
 Garcia Canyon 326–327, 331, 332, 333  
 geocentric axial dipole, Holocene 253, 256  
 geodynamo processes 261, 262  
 geology  
 Guide Basin 133–137  
 Itararé Group 357–358  
 Jiuquan Basin 174, 177  
 Lake Kalimpaa 247–248  
 Monte Cagnero 81–82  
 Nankai Trough 193  
 ODP Hole 647, Labrador Sea 30–31  
 ODP Hole 711A, Indian Ocean 99–100  
 Pringle Falls 262–263  
 Stirone section 310–312  
 Tibetan Plateau 150, 151–154  
 Umbria–Marche 112  
 geomagnetic excursions 4, 5, 6  
 Oligocene–Miocene 24–26  
*see also* excursion  
 Geomagnetic Instability Time Scale,  
 defining excursions 275  
 Geomagnetic Polarity Time Scale (GPTS) 1, 2, 89, 279  
 Guide Basin 138, 140  
 Jiuquan 180, 181  
 Nankai Trough 229  
 ODP Hole 711A 99, 106–107  
 Site U1333 21, 24  
 Stirone section 315, 318  
 Tibetan Plateau 158, 160, 161  
 geomagnetic pole paths 272–273  
 geomagnetic reversals, discovery of 1–3  
 GITS *see* Geomagnetic Instability Time Scale  
 glacial changes and anhysteretic remanent  
 magnetization 326  
 glacial–interglacial periodicities 363  
 glaciation, Gondwana 355  
 glaciogenic rhythmites 357  
 glaciomarine deposition 358  
 Global boundary Stratotype Sections  
 and Points (GSSP) 375, 377, 383  
 Capitanian–Wordian 376, 383–385, 387, 390, 392  
 Eocene–Oligocene boundary 81  
 Kungurian–Roadian 376, 382, 386, 391, 392  
 Rupelian–Chatian 82, 85, 121  
 Global Positioning System (GPS) 6, 168–169, 173  
 global sequence boundary 328  
 global stratigraphy 377–378  
 global warming 355  
 Gloria Drift 30  
 Gondwana glaciation 355  
 Gondwana I Supersequence 356, 357  
 GPS *see* Global Positioning System  
 GPTS *see* Geomagnetic Polarity Time Scale  
 GRA *see* gamma-ray attenuation  
 grain size 253, 265, 289, 309, 330  
 grain size and magnetization 196  
 grain size, experiment 280, 282, 283, 287  
 granulometry 331, 358  
 gravel composition 162, 163, 164  
 gravity collapse 149  
 Great Barrier Reef (outer), marine sediments 279, 281  
 greenhouse gases 81  
 gregite 315, 321  
 GSSP *see* Global boundary Stratotype Sections and Points  
 Guadalupian Mountains National Park 375  
 Guide Basin, NE Tibet, magnetostratigraphy  
 3D analysis 138–140, 142  
 age control 138  
 depositional environment 135, 145  
 geology 133–137  
 methods 137  
 rotation 186  
 sedimentary facies 142–146  
 sedimentation rates 138, 139, 145, 146  
 gypsum 154, 160, 161, 164
- Hallstatt solar cycle 365–367, 370  
 harmonic features 363, 365, 370  
 Heinrich warming events 367, 370  
 hematite 157, 178, 197, 224  
 Hexi Corridor Basin 149, 151, 152, 153, 167  
 Hexi Corridor, rotation 173–174, 183, 186  
 Hocke's estimator 301  
 Holocene (latest) dating 247, 257  
 Hongshuiba, rotation study 174, 177, 178,  
 180, 183, 185  
 Hopkinson Peak 287  
 hot-house fluctuations 367

- hypothermals 73  
hysteresis loop parameters 224, 228, 229  
granulometry 16, 18, 26, 103–105, 264–265, 266  
measurements 100, 196, 250, 282, 283, 284  
Milankovitch cycles 330, 331
- ice-house, Cenozoic 8  
Iceland Basin, excursions 273, 275  
Icelandic Magmatic Province, pole analysis 302–303, 305  
ice-sheet development 321  
ice-sheet Permo-Carboniferous 357, 358  
illite 385  
ilmenite 224  
inclination *Fig 10* opposite page 56  
Holocene 252, 255, 256  
Miocene–Pliocene 196, 197, 199, **223**, 226  
Oligocene–Miocene 21, 22–23, 24  
Pleistocene 287, 288–289  
Pliocene–Pleistocene 266–269, 270–271  
inclination, Cretaceous magma flows 296  
integrated magnetobiostratigraphy 50, 52, 54, 55  
integrated magnetostratigraphy 8, 29, 79, 97, 111  
Integrated Ocean Drilling Program (IODP) 13, 14  
322 Seismogenic Zone Experiment Expedition 191–241  
325 Hole M0058A magnetic experiments 280–287, 289  
Site U1333 (Pacific) 17–20, 21, 22–23  
*see also* Ocean Drilling Programme  
intensity 4–6  
outer Great Barrier Reef 287, 288–289  
Pringle Falls 262, 267, 269–271  
*see also* palaeointensity  
International Commission on Stratigraphy 377  
International Union of Geological Sciences 377  
IODP *see* Integrated Ocean Drilling Program  
IRM *see* isothermal remanent magnetization  
iron sulfide minerals 315, 316, 321  
isostatic rebound 149, 151  
isothermal remanent magnetization 3, 7  
Cupido Formation Mexico 330, 331  
IODP Site U1333 15, 16  
Jiuquan Basin 179  
Lake Kalimpa 250, 252  
Nankai Trough 196, 199, 223–224, 226  
ODP Hole 647A 34, 35  
ODP Hole 711A 100, 102, 107  
Pringle Falls 264–265  
Stirone section 312, 313, 315, 316  
Itararé Group, geology 357–358  
Itu rhythmites, Carboniferous 358, 360–366, **367–369**
- jack-knife analysis 159, 160  
Jiuquan Basin, Neogene rotation 173–187  
depositional environment 181  
geology 174, 177  
sections 178, 180, 183, 185–186  
Jiuquan, foreland basin 152, 163, 165, 166, 169
- K1 *see* spectral analysis of maximum axis of anisotropy of magnetic susceptibility  
K–Ar age 262  
Kii Peninsula, earthquakes 192  
Kope Formation, Milankovitch cycles 341–351  
composite reference section 345, 348–351  
lithostratigraphy 342–344  
K–Pg *see* Cretaceous–Palaeogene  
K–T boundary 111, 117, 344  
Kungurian–Roadian global stratotype 376, 382, 386, 391, 392
- laboratory methods *see* methods/laboratory  
Labrador Sea 29, 30, 72  
lacustrine sediments 262–263, 265, 266, 275  
Lake Kalimpa, radiocarbon chronology evaluation 245–257  
age-depth model 250, 254–257  
archive 247  
chronology 250, 252–253  
climate and geology 247–248  
materials and methods 248–250  
palaeomagnetic data 253–254  
Laojunmiao section 174, 177, 178, 183, 185  
Laschamp Excursion 288, 289, 290  
Last Glacial Maximum 279, 280  
latitude, high to low integration 29–74  
latitude/longitude, secular variation 293–295, 297–298, 304
- limestone  
magnetic susceptibility 378, 384  
magnetostratigraphy susceptibility 379, 382  
thermomagnetic susceptibility 386  
Ordovician 343, 345, 346, 348, 350  
loess 135  
low-field magnetic susceptibility 309–321, 377, 380  
low-temperature properties 224, 230, **231**  
lysocline 73
- Madingley Rise 97  
magnetic foliation 357  
magnetic granulometry 331  
magnetic lineation 357  
magnetic measurement procedure 195–196  
magnetic mineralogy 6  
Cupido Formation 330–331  
Guadalupe Mountains 384–385, 386  
Northern Apennines 309, 313, 315, 321  
magnetic palaeointensity 4–6  
*see also* intensity  
magnetic polarity record, Nankai Trough  
Hole C0011B **200–211**, 229–230, **233–235**  
Hole C0012A **212–223**, 236, **237–239**  
magnetic polarity reversal stratigraphy  
ODP Hole 647A 47, 50–67  
Stirone section 311, 313  
Magnetic Reversal Polarity Timescale *Fig 10*  
opposite page 56  
magnetic susceptibility  
experiment 280, 282, 283  
Ordovician 341–344  
measurements 345–346  
*see also* anisotropy of magnetic susceptibility  
magnetite 85, 102, 105, 287  
Apennines 315, 316, 321  
Indonesia 254  
Mexico, NE 326, 329, 338  
Nankai Trough 196, 223, 224  
Oregon 266  
Pacific sediments 18, 20, 26  
Tibet (NE) 157, 178

- magnetite, Curie temperature 264, 265, 275, 380, 385  
 magnetite, loss of 344, 378  
 magnetization saturation (Ms)  
   Lake Kalimpa 250  
   Pringle Falls 264, 266  
   outer Great Barrier Reef 282, 283, 284–287  
 magnetization saturation remanence (Mrs)  
   Lake Kalimpa 250  
   Pringle Falls 266  
   outer Great Barrier Reef 282, 283, 284–287  
 magnetobiochronological summary 50, 52, 54, 55  
 magnetobiostratigraphy, Eocene–Oligocene, Monte Cagnero 79–92  
   age calibration refinement 91–92  
   geomagnetic polarity time scale 89–90  
   methods 83–84  
   polarity 84–85  
   sedimentation rate 90–91  
 magnetobiostratigraphy, Palaeogene pelagic succession 111–128  
 magnetosomes 331  
 magnetostratigraphic analysis  
   3D 138–140, 142  
   Stirone section 312  
 magnetostratigraphy  
   and deformation 149–169  
   basin analysis 133–146  
   conference volume 7–8  
   equatorial Pacific 17–20, 21, 22–23  
   Indian Ocean site 97–107  
   methods 137  
   polarity time scale 3–4  
 magnetostratigraphy susceptibility, Middle Permian stratotype  
   biostratigraphy 376–377  
   climate 379  
   floating-point time scale model 387–391  
   Fourier transform and multi-taper analysis 380–382, 387, 388–389, **390**  
   general comments 378, 380  
   global stratigraphy 377–378  
   graphic comparison 385–387, 390  
   sampling and measurement 380–382  
   sedimentary rocks 378–379  
 magnetostratigraphy susceptibility, Ordovician 345, 346–349, 351  
 magnetotactic bacteria 326, 331  
 magnetotelluric data 168  
 mantle 151, 168  
 Massignano, pelagic succession 112, 113, 116, 119–120  
 maximum angular deviation, Lake Kalimpa 248, 252, 253–254  
 McElhinny's tilt test 159, 179  
 MECO *see* Middle Eocene Climatic Optimum  
 median destructive field, Lake Kalimpa 253–254  
 Mediterranean, circulation 321  
 meteorite impact 344  
 methane expulsion 312  
 methods/laboratory  
   chronology evaluation 248–250  
   cyclostratigraphy 194–197, 330, 312–315  
   magnetobiostratigraphy 83–84, 112–114  
   magnetostratigraphy 100, 137, 194–197  
   polarity excursions 263–269  
   rock magnetism 264–269, 280–287, 289, 329–330  
   rotation 177  
   spectral analysis and anisotropy 358, 360  
   thermomagnetic susceptibility 380  
   time series analysis 344–346, 379–382  
   uplift and deformation 156–157  
   virtual geomagnetic pole paths 294–298  
 microfossil bioevents **40–42**  
 Middle Eocene Climatic Optimum (MECO)  
   Indian Ocean 98, 99, 107  
   Italy 81  
   Labrador Sea 52, 68, 69, 71, 72, 73  
 Middle Permian, Guadalupian Series, stratotype 375, 377  
 mid-ocean ridges 1  
 Milankovitch bands 379, 381, 387, 392  
 Milankovitch cycles  
   Cretaceous 313, 315, 317 *see also below*  
   Permo-Carboniferous 355, **367, 369**  
 Milankovitch cycles, Lower Cretaceous 325–338  
   anhysteretic remanent magnetization 331–337  
   data and methods 329–330  
   magnetic mineralogy 330–331  
 Milankovitch cycles, Upper Ordovician 341–351  
   composite reference section 348–351  
   lithostratigraphy 342–344  
   magnetic susceptibility 341–344  
   measurements 345–346  
 missed beat, peritidal 325, 337  
 molasse 144, 152, 186  
 monsoon 245  
   African 320–321  
   and isostatic rebound 149  
 Monte Cagnero, Eocene–Oligocene section 79–92  
   biostratigraphy 83–84, 85, 87–89  
   geomagnetic polarity time scale 89–90  
   palaeomagnetism 83, 84–85  
   polarity zonation 84–85, 87  
   sedimentation rate 90–91  
   stratigraphy 81–82, 112, 113, 116, 118, 119–121  
 multi-proxy investigations, Lake Kalimpa 247, 254, 256  
 Multisensor Core Logger 280, 282  
 multi-taper spectral estimation 380–382, 388–389, **390**  
 Multi-Taper results 347  
 Nankai Trough, Expedition 322 IODP 192, 193  
   Hole C0011B 194, 224–232, 241  
   age datum **233–235**  
   polarity **200–211**, 229–230  
   Hole C0012A 224–226, 229–231, 240, 241  
   age datum 236, **237–239**  
   polarity **212–222, 223**  
 Nankai Trough Seismogenic Zone Experiment (NanTroSEIZE)  
   age-depth model 229–230, 232–240  
   data analysis 196–197  
   depositional environment 194–195  
   geology 193  
   laboratory methods 194–197  
   palaeomagnetic results 197–199, **200–222, 223**  
   rock magnetic characterization 199, 223–226  
   stability tests 226–228, **231**

- nannofossil ooze 15–16, 102
- nannofossils  
Miocene 194, 232, **233–235**, **237–239**, 240
- nannofossils, Palaeogene  
Monte Cagnero 83–84, 88–89, 107  
ODP Hole 647A 31–32, 34, **36–37**, **45–47**, 65  
Umbria–Marche succession 113–127
- natural remanent magnetisation (NRM) 3  
deep sea sediments 15, 17–18, 32, 100–101, 102  
Guide Basin 137  
Lake Kalimpa 248, 252  
Monte Cagnero 83, 84  
Nankai Trough 197, 198  
outer Great Barrier Reef 282, 283, 287, 288  
Pringle Falls 264–269  
Stirone section 313, 314
- Neogene 318, 319  
Neogene basin infill 134  
Neo-Tethys gateway 81, 99  
Neo-Tethys Sea 152  
Newberry volcano 262, 263, 275  
Nongchunhe Valley 136, 138, 140, 142, 145, 146  
North Atlantic Ocean 29, 30  
NRM *see* natural remanent magnetization  
Nyquist frequency 296, 297
- obliquity orbital cycle  
Cretaceous 326, 347  
Late Neogene 310, 315, 317, 318, 319, 320  
Mid Permian 387, 392  
Ordovician 348, 349, 350, 351  
Permo-Carboniferous, Brazil 360, 363
- ocean circulation 30, 320–321
- Ocean Drilling Programme, Hole 647A 29–74  
age model and errors 38, 39, **40–42**  
age model and new datum **58–64**, 67–68, 71–73  
biostratigraphy 34–38, 39–47, **48–49**  
chronology 31–32  
geology 30–31  
magnetic polarity reversal stratigraphy 47, 50–67  
palaeoceanography 72–73  
palaeomagnetism 32–34  
sedimentation rates 68–71  
seismic line 31  
spectral analysis 38, 71–72  
stable isotopes 38, 72
- Ocean Drilling Programme, Hole 711A 97–107  
age-depth model 105, 107  
biostratigraphy 105–206  
geology 99–100  
methods 100  
palaeomagnetic polarity zonation 100–102  
rock magnetic properties 102–105  
sedimentation rate 106, 107  
*see also* Integrated Ocean Drilling Program
- Oceanic Anoxic Event 328, 335, 338
- oceanic magnetic anomalies 1
- ODP *see* Ocean Drilling Programme
- Olduvai Chron 312, 316
- Oligocene–Miocene boundary 23, 26
- Oligocene–Miocene magnetostratigraphy 13–26
- orbital cycles, correlation 315–317, 318
- orbital eccentricity 313, 326, 335, 337, 338
- orbital frequency 348
- orbital variability 309  
Ordovician 347, 348, 350, 351
- oxygen isotope 72, 97–99, **249**, 252  
and climate change 79, 81
- Pacific Equatorial Age Transect 13
- Pacific, equatorial, deep-sea investigation 13–26
- palaeoceanographic events, correlation 29–72  
age model 72–74
- palaeoceanography 72–73
- palaeoclimate 309  
Eocene–Oligocene 97–99  
Permo-Carboniferous 365, 367  
palaeoclimate proxy 326, 357, 370  
palaeoclimate, astronomical forced insolation 7
- palaeocurrent direction 163, 164, 358  
and anisotropy of magnetic susceptibility 357
- palaeo-depth 31, 82, 97
- palaeoenvironmental studies 245, 357
- Palaeogene, oceanic red beds 120, 128
- Palaeogene, pelagic composite succession 111–128  
integrated stratigraphy 120, 121–128
- palaeogeographic reconstruction 98, 133, 334
- palaeointensity 4–6, 8  
Lake Kalimpa 247, 254, 255, 256  
polarity excursions 262  
*see also* intensity
- palaeomagnetic  
biostratigraphic age datum 39, **233–235**, **237–239**  
chronology evaluation 253–254  
direction summary **175–176**, **182–184**  
high resolution 247  
polarity zonation 100–102  
reference directions, Eurasia **184**  
sampling 194–195  
secular variation 247, 257  
sediment data **200–223**
- palaeomagnetic dating 133, 151, 158–161, 185–186  
ODP Hole 647A 32–68  
IODP Nankai Trough 232–240
- palaeosecular variation, Lake Kalimpa 247, 253
- paramagnetic grains 330, 367, 378, 379, 380
- paramagnetic phases 343, 344, 346
- Paraná Basin, magnetism and sedimentary cycles 355, 357–358
- Paraná Magmatic Province 295
- pDRM *see* post-depositional remanent magnetization
- pelagic succession 81–82, 111–128
- periodogram 296, 298–299, 301, 304
- peritidal facies 325, 328, 337
- Permo-Carboniferous 360, 363, 367
- Philippine Sea Plate 192, 193
- plate boundary slip 191–192
- plate-driven eustasy 346
- playa 154, 161, 164  
Pliocene–Pleistocene 310, 315, 317–321  
Pliocene–Pleistocene, Stirone section 309–321
- polarity 1–3  
Hole C0011B **200–211**, 229–230, **233–235**  
Hole C0012A **212–223**, 236, **237–239**
- polarity and inclination 21, 23
- Polarity Chron, reversal boundary 73

- polarity excursions 4–6, 24–26, 262, 273, 275, 288–290  
*see also* excursion
- polarity interval 193, 196, 226, 229, 236
- polarity reversal 8, 261, 279, 294, 312, 317  
 boundaries 310  
 data **22**, **23**  
 theory of 3–4, 5  
 timescale *Fig 10* opposite page 56
- polarity zones  
 Guide Basin 138, **139**  
 Tibetan Plateau 158–160
- pole paths 272–273  
 comparative analysis 302–303, 305  
 Early Cretaceous lava, Brazil 293–306
- Popper-Bayes paradigm 295
- post-depositional remanent magnetization 3, 312, 313, 315, 316
- precession  
 Cretaceous, Lower 326, 330, 335–336  
 Mid Permian 387, 392  
 Ordovician 347, 348, 350, 351  
 Permo-Carboniferous 360, 363, 367  
 Pliocene–Pleistocene cycle 310, 315, 317–321
- Pringle Falls, excursion 261–275  
 age 263, 273–274  
 geology 262–263  
 laboratory experiments 263–269  
 virtual geomagnetic pole paths 269–274
- pseudo-single domain 16, 18
- pyrite 343, 344, 378
- pyrrhotite 321
- Qilian Shan, magnetostratigraphy 150, 151–154, 163–167
- radiocarbon chronology, evaluation 245–257
- radiocarbon dating 280, 288  
 Lake Kalimpa 247, **249**
- radiolarian chert 112
- radiometric age 274  
 Ar/Ar 275, 288, 294  
 K–Ar 262  
 U–Th 288  
 U–Th/He 151
- red beds, Palaeogene 120, 128, 134, 180
- reef carbonate 287–288
- relative palaeointensity 8
- remanent magnetization 3, 179, 378, 379
- results 313–315
- reversal *see* polarity
- rhythmites, Carboniferous–Permian 355–370
- rigid block 168, 169, 173
- Rio do Sul rhythmites, Permian 358, 359, 360–363, **367–369**
- RM *see* remanent magnetization
- Roadian, global stratotype 376, 382, 383, 391, 392
- rock magnetic characterization 194, 199, 223–226
- rock magnetic cyclostratigraphy, Pliocene–Pleistocene  
 age model 309–311, 317–320  
 climate cycles encoding 320–321  
 geology 310–312  
 methods 312–315  
 orbital cycles correlation 315–317, 318
- rock magnetic experiments 179  
 IODP 325 Hole M0058A 280–287, 289  
 Pringle Falls 264–269
- rock magnetic properties 17–20, **227**  
 ODP Hole 711A 102–105
- rotation, Neogene 173–187  
 direction of 183, 185–186  
 laboratory methods 177  
 palaeomagnetic results 177–180, 183, 185–186  
 sample collection 174  
 vertical axis 173, 174
- run-off 320, 321
- salinity 320–321
- sample collecting  
 directional geomagnetics 263–264  
 magnetic cyclostratigraphy 137, 329  
 magnetostratigraphy 156–158, 194–195
- sapropels 312, 319, 320, 321
- saturated isothermal remanent magnetization  
 Cupido Formation 331  
 Lake Kalimpa 250, 252  
 outer Great Barrier Reef 282
- saturation remanent magnetization ( $M_r$ ) 196, 264
- sea-level change 279, 321, 328, 343, 344
- sea-level oscillation 325, 333, 336, 337
- secular variation 5, 293–295, 297–298, 302–304  
 Lake Kalimpa 247, 253
- sediment provenance 146
- sediment, low-temperature rock magnetic measurements **231**
- sedimentary facies, Guide Basin 142–146
- sedimentary rock, geomagnetic variations 293
- sedimentary rock, magnetic susceptibility 378–379
- sedimentation rate 23  
 Guadalupe, Texas 382, 385–387, 390, 391, 392  
 Guide Basin 138, **139**, 145, 146  
 Kope Formation/Ordovician 342, 348–351  
 Lake Kalimpa 253, 256–257  
 Monte Cagnero 90–91  
 Nankai Trough 193, 232, 236, 240, 241  
 ODP Hole 647A **60**, 68–71  
 ODP Hole 711A 106, 107  
 Stirone section 310, 317, 318, 321  
 Tibetan Plateau 163, 164, 166  
 Umbria–Marche Basin 120, 124, 125
- sedimentation rate  
 red beds 128  
 rhythmites 363, **367**, 369, 370
- seismic line, NW Atlantic 31
- seismic moment tensor analyses 173
- sequence stratigraphy, Cupido Formation 333, 335, 337–338
- Serra Geral lavas 295, 297, 298, 302, 303
- shipboard palaeomagnetic measurements 197, 198, **200–223**, 232, 240
- shortening rate 168–169, 186
- siderite 343, 344, 378, 385
- SIRM *see* saturated isothermal remanent magnetization
- Skálamælifell Hill lavas 288, 290
- slip plate boundary 191–192
- soft ranges 167, 168, 169
- soft-sediment, susceptibility 282, 283–285, 287, 289
- solar cycle periodicity 365–367

- spectral analysis  
 Cupido Formation, Mexico 333, 334, 337  
 Guadalupian, Texas 380–381, 388–389  
 Kope Formation, Kentucky 348  
 ODP Hole 647A 38, 71–72  
 palaeoclimate proxy 356, 357, 366, 370  
 rhythmites, Brazil 355, 356, 360, 362, 363, 366–370
- spectral analysis, magnetostratigraphy 294, 296–303  
 artefacts 306
- spline function 345, 380, 381, 382
- stability tests, magnetic 226–228, **231**
- stable isotopes, ODP Hole 647A 38, 72
- Stirone section, age model 317–320
- storm deposits 343
- Stratotype Canyon 376, 377, 382, 385–387, 389–392
- strike slip, Jiuquan Basin 186
- subduction zone 192, 193
- Sunan, magnetostratigraphy 154, 156, 158, 159, 160  
 sedimentology 161–163  
 tectonics 164, 166
- susceptibility and temperature 282, 285, 287
- synthetic data series 299–301  
 real data comparison 303
- T3 Climate Event 389
- Tahiti reef sequence 288
- taxon **40–49**, 87–89, 105–106
- tectonics and palaeomagnetism 6, 8
- temperature (low-) and magnetics 329
- temporal resolution 309
- tephra 262
- Tethyan reference age model 124–125, 126–127
- Tethys Block 168
- Tethys Ocean 112, 152  
 closure 81
- Texas (West) sections 376
- thermal demagnetization  
 Cupido Formation, Mexico 330  
 Guide Basin 137  
 Jiuquan Basin, China 177, 178  
 Monte Cagnero, Italy 83, 85, 86  
 Nankai Trough 193, 195, 197, 198  
 ODP Hole 647A 34, 35  
 Stirone section 312, 314, 315  
 Tibetan Plateau 156, 158
- thermomagnetic curve 225, 265
- thermomagnetic heating 85, 86–88
- thermomagnetic susceptibility measurement 379, 380, 386
- thermoremanent magnetization 3
- Tibetan Plateau (NE) 149–169  
 geology 149–156  
 magnetostratigraphy 158–161  
 palaeocurrents 164  
 palaeomagnetic direction **175–176**, **182–184**  
 sampling and measurement 156–158  
 sedimentology 161–163  
 shortening 168–169  
 uplift and tectonics 163–167, 173–174
- time calibration and spectral analysis 360
- time calibration to astronomical parameters 363
- time control, high resolution 309
- time, uneven sampling 293, 294, 296
- time-series analysis 380–382, **390**  
 methods, magnetic cyclostratigraphy 330  
 Middle Permian 387, 392  
 Milankovitch cycle 313, 335, 342, **346**, 348
- titanomagnetite 228
- titanomaghemite 102, 105, 107, 197, 224, 228  
 Pringle Falls 264, 275
- tree rings, Holocene 365
- U-channel methods 16–18, 282, 286, 288, 289
- Umbria–Marche Basin 111–128  
 age-depth models 114, 122–127  
 geology 112  
 methods 112–114  
 sections, integrated stratigraphy 115–128
- unconformity 73  
 Middle Eocene *Fig. 10* opposite page 56  
 Tibetan Plateau 156, 160, 161, 163, 166–167
- uplift, Jiuquan Basin 165, 186
- uplift, Tibetan Plateau 173–174
- U–Th dating 288
- U–Th/He dating 151
- variable field translation balance 282
- varvitos *see* rhythmite
- Verwey transition 224, 228, 329
- VGP *see* virtual geomagnetic pole paths
- virtual geomagnetic pole 4  
 oscillatory trajectories 304
- virtual geomagnetic pole paths 269–274  
 Brazilian lavas 293–306  
 deep sea sediments 19, 21, 22, 24  
 Guide Basin 137, 138, 140–141  
 Jiuquan Basin 177, 181  
 Pringle Falls 269–274  
 Stirone section 311, 312, 313  
 Tibetan Plateau 157, 158, 160, 161
- viscous remanent magnetization 3
- volcanic magnetostratigraphy 293–294
- volcanism, Tibetan Plateau 149, 151
- Wanda Swamp 245, 246, 254
- warming event 72, 73
- wavelength in virtual geomagnetic pole trajectories  
 293–306  
 dataset 294  
 periodogram analysis 298–299  
 phase determination 301–302  
 spatial behaviour 303–304  
 spectra stability 301  
 study method 294–298  
 testing and comparison 299–306
- Wenshushan, rotation study 174, 177, 180, 183, 185
- Wordian, global stratotype 376, 383–385, 387, 390, 392
- Yellow River, erosion 146
- Yumu Shan Fault (Northern) 150, 152, 154, 155, 166–167
- Yumu Shan  
 magnetostratigraphy 150, 152–158, 160–161  
 rotation study 174, 177, 180, 183, 185  
 sedimentology 163  
 tectonics 164, 165, 166

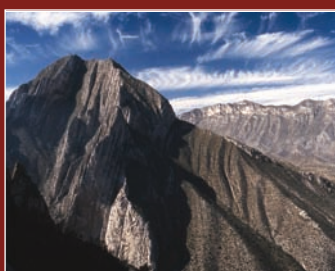


# Magnetic Methods and the Timing of Geological Processes

Edited by

**L. Jovane, E. Herrero-Bervera, L. A. Hinnov and B. A. Housen**

Magnetostratigraphy is best known as a technique that employs correlation among different stratigraphic sections using the magnetic directions defining geomagnetic polarity reversals as marker horizons. The ages of the polarity reversals provide common tie points among the sections, allowing accurate time correlation. Recently, studies of magnetic methods and the timing of geological processes have acquired a broader meaning, now referring to many types of magnetic measurements within a stratigraphic sequence. Many of these measurements provide correlation and age control not only for the older and younger boundaries of a polarity interval, but also within intervals.



Thus, magnetostratigraphy no longer represents a dating tool based only on geomagnetic polarity reversals, but comprises a set of techniques that includes measurements of geomagnetic field parameters, environmental magnetism, rock-magnetic properties, radiometric dating and astronomically forced palaeoclimatic change recorded in sedimentary rocks, and key corrections to magnetic directions related to geodynamics, palaeocurrents, tectonics and diagenetic processes.

**Visit our online bookshop:** <http://www.geolsoc.org.uk/bookshop>

**Geological Society web site:** <http://www.geolsoc.org.uk>



## **Cover illustration:**

View looking NW from the mountainside entrance to Grutas de Garcia (Garcia Caverns) within the Potrero anticline, northeastern Mexico. See Hinnov *et al.* p.325 for more information.

Photograph by David Anastasio.